coordinated sites,[9,10] thus reducing $4\pi M$. Using a single-crystal YIG-Ga sphere with a $4\pi M$ of 1000 gauss the measured frequency octave is from 935 to 1870 Mc at room temperature. A limiter has been constructed to operate at 1300 Mc which has an insertion loss of 0.7 db, a limiting power of 10μ watts, and a curve similar in all respects to that of Fig. 2. The 0.7-db insertion loss could be reduced by using a larger sphere.

The response of the limiter to pulses of RF energy always shows a spike on the leading edge. The reason for this is that the subsidiary resonance does not build up instantaneously. The time of build up is associated with the relaxation time of the RF magnetization. When a pulsed RF signal is applied, ferromagnetic resonance occurs and the angle of precession of magnetization increases, opening up to a value $>\theta_{crit}$. Eventually subsidiary resonance occurs and θ decays to its final value of θ_{crit}.

Fig. 3 shows the spike for a sequence of pulses of RF energy. The build-up time of subsidiary resonance becomes shorter as the power is increased [see Suhl's (24)]. For RF power levels moderately in excess of the limiting power, we were able to integrate the area under the spike and show that it remains constant. At higher power levels it was not possible, however, to show definitely that the spike energy remains constant.

We should like to thank R. C. LeCraw for helpful discussions on these experiments, J. J. Kostelnick for suggestions on the structure, S. Geller for many discussions of his work on substituted garnets, and J. W. Nielsen and R. C. Linares for the growth of all the crystals used in these experiments.

F. J. Sansalone
E. G. Spencer
Bell Telephone Labs., Inc.
Murray Hill, N. J.

[9] M. A. Gilleo and S. Geller, "Magnetic and crystallographic properties of substituted yttrium iron garnet, $3Y_2O_3 \cdot XM_2O_3 \cdot (5-X)Fe_2O_3$," *Phys. Res.*, vol. 110, pp. 73–78; April, 1958.
[10] S. Geller, "Magnetic interactions and distribution of ions in the garnets," *J. Appl. Phys*, vol. 31, pp. 30–37S; May, 1960.

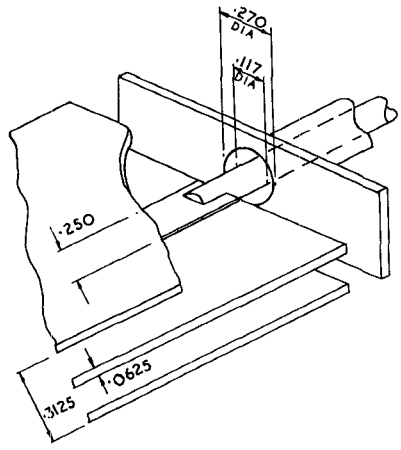

Fig. 1—Standard stripline-to-coaxial line 50-ohm transition.

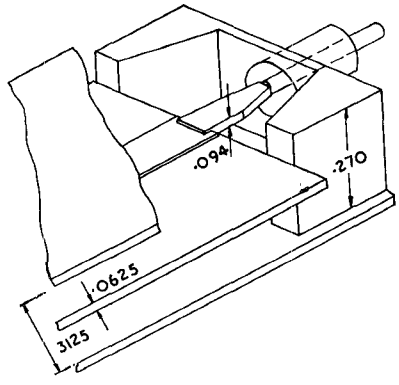

(a)

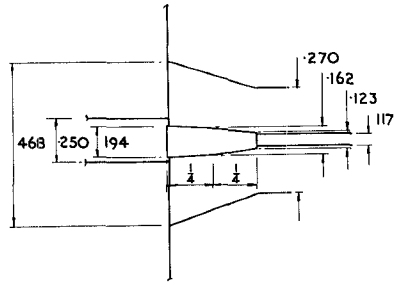

(b)

Fig. 2—Stripline-to-coaxial line tapered transitions using rectangular line.

New Coaxial-to-Stripline Transformers Using Rectangular Lines*

The most common form of coaxial-to-stripline transition consists of a simple in-line butt joint, as described by Barrett.[1] A typical transition between a 50-ohm high-Q triplate and a standard N-type connector is shown in Fig. 1. This gives a VSWR <1.15 at frequencies up to 7000 Mc deteriorating to 1.25 at higher frequencies up to 11,000 Mc. While these results are acceptable for many types of stripline components and assemblies, it was felt that the design of a better transition would be necessary in order both to test and to maintain the performance of high grade components (*e.g.*, hybrids, directional couplers, and filters) and to avoid the manufacture of a special stripline standing-wave detector.

The conventional transition (Fig. 1) is not perfectly matched because the fringing field of the stripline is intercepted by the outer conductor of the coaxial line, in addition to the disparity of dimensions between the inner conductors of the two lines.

A diagram of a well-matched transition is shown in Fig. 2. In this, the side walls at the start of the transition from the stripline end are positioned sufficiently far away from the stripline to avoid discontinuities, a constant 50-ohm impedance is maintained through the transition to the coaxial line, and there are no large dimensional discontinuities. The VSWR of this transition, as deduced from measurements of two such transitions back-to-back cascaded with terminating N-type connectors and a matched load, is probably better than 1.02 at all frequencies up to the highest measured frequency of 11,000 Mc; and, in fact, it is probable that the transition does not deteriorate the VSWR of the N-type connector.

A cross section through the transition in a plane perpendicular to its axis is shown in Fig. 3, and takes the form of a rectangular line. It was necessary to derive a formula for the characteristic impedance of the rectangular line, and this was obtained in the form

$$Z(w/b, t/b, s/b) = \frac{94.15}{\sqrt{\epsilon}\left[\dfrac{w/b}{1 - t/b} + C_{f0}'(t/b, s/b)\right]}, \quad (1)$$

where

$$C_{f0}'(t/b, s/b) = C_{f0}'(0, s/b) + \epsilon t/s. \quad (2)$$

Here ϵ is the *relative* dielectric constant of the dielectric medium of the line, and $C_{f0}'(0, s/b)$ is the fringing capacitance of the rectangular line as given by Cohn[2] in the form

$$C_{f0}'(0, s/b) = \frac{2\epsilon}{\pi} \log\left[1 + \coth(\pi s/2b)\right]. \quad (3)$$

A graph of $C_{f0}'(0, s/b)$ as a function of s/b is plotted in Fig. 7 of Cohn's paper.

Eq. (1) gives a good approximation to the impedance of the line, valid for $s/t \leq 5$, a condition which is always true in the case of the transition shown in Fig. 2.

More general formulas for the characteristic impedance of rectangular lines have now been derived by Chen[3] with the inde-

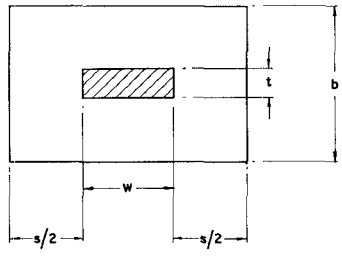

Fig. 3—The rectangular line.

* Rece ved by the PGMTT, February 3, 1961.
[1] R. M. Barrett, "Etched sheets serve as microwave components," *Electronics*, vol. 25, pp. 114–118; June, 1952.
[2] S. B. Cohn, "Shielded coupled-strip transmission line," IRE Trans. on Microwave Theory and Techniques, vol. MTT-3, pp. 29–38; October, 1955.
[3] T. S. Chen, "Determination of the capacitance, inductance and characteristic impedance of rectangular lines," IRE Trans. on Microwave Theory and Techniques, vol. MTT-8, pp. 510–519; September, 1960.

pendent suggestion that such lines might be used as a transition between coaxial and strip-transmission lines.

It is worth noting that an exact formula has been derived for the characteristic impedance of the rectangular line with an inner conductor of zero thickness ($t=0$ in Fig. 3). This is given approximately by Chen in his equation (23), which may be written in the following revised form to conform with the notation of Fig. 3:

$$Z(w/b,\ 0,\ s/b) = \frac{94.15}{\sqrt{\epsilon}[w/b + 2/\pi \cdot \log(1 + \coth \pi s/2b)]}. \quad (4)$$

Eq. (4) is in fact identical to (1) with $t=0$.

The conformal transformation of one-half of the rectangular line is shown in Fig. 4. The transformation from the z plane to the t plane is standard, and is given by

$$t = \mathrm{sn}\,(Bz, k_1) \quad (5)$$

which upon use of the boundary conditions gives

$$t = \mathrm{sn}\left[\frac{2K(k_1)\cdot z}{w+s},\ k_1\right] \quad (6)$$

and

$$b/(w+s) = K'(k_1)/K(k_1), \quad (7)$$

where $K(k_1)$ is the complete elliptic integral to modulus k_1, and $K_1'(k_1)$ is the complementary integral. The transformation of the t plane to the χ plane, where the field pattern is regular, is also standard and is given by

$$t = k\ \mathrm{sn}\,(\chi, k). \quad (8)$$

The impedance of the half line is thus given by $Z=376.6\ K'(k)/2K(k)$, resulting in the formula for the impedance of the complete rectangular line,

$$Z = 94.15\,\frac{K'(k)}{K(k)}. \quad (9)$$

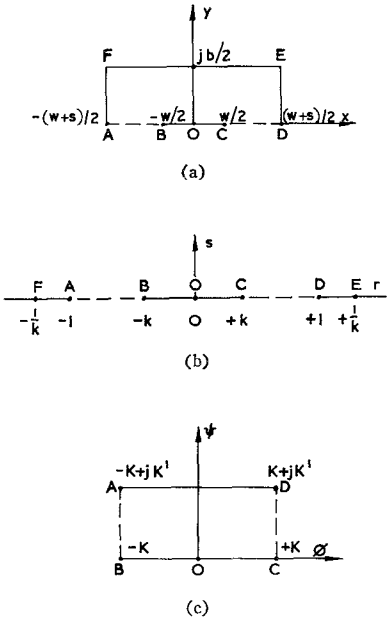

Fig. 4—Conformal transformation of the rectangular line with zero thickness inner conductor. (a) Z plane (b) t plane (c) X plane.

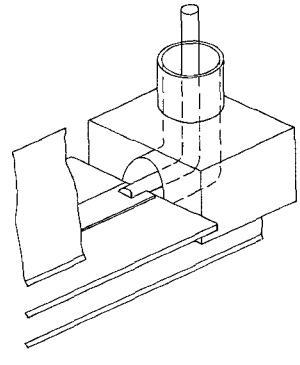

Fig. 5—Right-angled stripline-to-coaxial line transition.

The relationship between k and k_1 is obtained from (6) by using the condition that $t=k$ when $z=w/2$, giving

$$k = \mathrm{sn}\left[\frac{w}{w+s}K(k_1), k_1\right],$$

i.e.,

$$\frac{w}{w+s}K(k_1) = F(k, k_1) = F(\theta, \phi), \quad (10)$$

where $F(k, k_1)$ is the incomplete elliptic integral of the first kind of argument k and modulus k_1. It is usual to put $k=\sin\phi$ and $k_1=\sin\theta$ since $F(\theta, \phi)$ is usually tabulated.

The procedure for determining the impedance of the line exactly from its parameters w, s, and b is thus to find the modulus k_1 from (7) and to substitute this into (10) to find ϕ and hence k, which is used in the impedance formula (9). In practice, it is found that this procedure is almost as simple as the calculation of (4), since the elliptic integrals have been well tabulated; and therefore, the exact procedure might always be adopted. It is seen that the approximate formula (4) breaks down badly as $s/b\to\infty$, since then the expression for the capacitance in the denominator reduces to that of a simple parallel-plate capacitor, there being no allowance for the fringing capacitance.

It is possible also to construct the stripline-to-coaxial line transition in a right-angled form as shown in Fig. 5, which depicts a simple butt joint followed immediately by a right-angled coaxial bend. The match of this transition is as good as that of the in-line version shown in Fig. 1. This form of transition, where the coaxial line output is normal to the ground plane is particularly useful in integrated assemblies. It is proposed to combine this form of transition with the tapered section to form a well-matched right-angled transition possibly equal in performance to the in-line transition as described above.

R. Levy
Mullard Res. Labs.
Surrey, England